Phase Transitions
Vol. 82, No. 4, April 2009, 344–355

Taylor & Francis
Taylor & Francis Group

Lattice anharmonicity and structural evolution of $LiBH_4$: an insight from Raman and X-ray diffraction experiments

H. Hagemann[a]*, Y. Filinchuk[b], D. Chernyshov[b] and W. van Beek[bc]

[a]*Département de Chimie Physique, Université de Genève, 30 quai E. Ansermet, CH-1211 Geneva 4, Switzerland;* [b]*Swiss-Norwegian Beam Lines at ESRF, BP-220, 6 rue Horowitz, F-38043 Grenoble, France;* [c]*Dipartimento di Scienze e Tecnologie Avanzate and Nano-SiSTeMI Interdisciplinary Centre, Università del Piemonte Orientale "A. Avogadro", Via V. Bellini 25/G, 15100 Alessandria, Italy*

(*Received 6 November 2008; final version received 22 December 2008*)

New *in situ* Raman and synchrotron X-ray diffraction data (between 300 and 400 K) in conjunction with separate temperature-dependent Raman data (between 7 and 400 K) are presented. The low-frequency Raman spectra show good agreement with theoretical values obtained previously using periodic DFT calculations. The temperature-dependent spectra reveal the presence of significant anharmonicity of librational modes neither predicted theoretically nor noted in previous experiments. The splitting of the internal deformation mode υ_2 (of *E* symmetry in the free ion) decreases continuously with increasing temperature, but drops abruptly at the first-order orthorhombic to hexagonal phase transition observed at 381 K. The temperature dependence of the linewidth of the internal deformation mode υ_2 reveals coupling to reorientational motions of the borohydride ion in the orthorhombic phase. The thermal evolution of both crystal structure and vibration frequencies agree with the phase diagram suggested by the Landau theory.

Keywords: Raman spectroscopy; hydrogen storage materials; X-ray diffraction; *in situ* experiments

1. Introduction

$LiBH_4$ is an important candidate for solid hydrogen storage. For the pure compound, the thermodynamics of reversible hydrogen storage is not favourable, but it has been shown in recent years that the combination of $LiBH_4$ with other compounds such as CaH_2 or MgH_2 allows to reduce the enthalpy difference associated with the release of hydrogen [1,2]. For this reason, it is important to understand in detail the properties of $LiBH_4$ as a function of temperature and pressure. In the past years, the crystal structure of $LiBH_4$ has been studied at different temperatures and pressures, and the complex phase transition scheme has been analysed [3–7].

At ambient pressure, $LiBH_4$ is orthorhombic (Pnma) and undergoes a first-order phase transition on heating at 381 K to a hexagonal high-temperature phase ($P6_3mc$). At ambient

*Corresponding author. Email: hans-rudolf.hagemann@unige.ch

ISSN 0141–1594 print/ISSN 1029–0338 online

DOI: 10.1080/01411590802707688
http://www.informaworld.com

temperature, a phase transition into a high-pressure phase (Ama2) is observed around 0.6 GPa, and a second transition at *ca* 18 GPa leads to a cubic phase (Fm-3m) [6].

The phonon modes in $LiBH_4$ and $LiBD_4$ have been studied before [8–11]. However, besides the very recent work by Racu et al. [11], a detailed temperature evolution of Raman lines is still not documented. In this work, we present new Raman data as a function of temperature in conjunction with synchrotron diffraction data. These vibrational data are discussed in conjunction with previous vibrational studies on $LiBH_4$ [8–11], and correlated with structural response to temperature together with the phase diagram suggested before on the basis of symmetry analysis [7].

2. Experimental

In situ synchrotron powder diffraction/Raman spectroscopy experiments have been carried out at the Swiss-Norwegian Beamlines at the European Synchrotron Radiation Facility between 300 and 400 K. The data were collected on a 0.5 mm glass capillary filled with polycrystalline $LiBH_4$ (Aldrich), using KUMA-6 diffractometer, Onyx $1K \times 1K$ CCD detector at a sample-to-detector distance of 120 mm, $\lambda = 0.70855$ Å. At each temperature point the capillary was rotated by 60° during the 60 s exposure time. The data were integrated with a Fit2D program (A. Hammersley, ESRF), using a calibration measurement of a NIST LaB_6 standard powder sample. Good estimates of $\sigma(I)$ were calculated with a local program by applying Poisson statistics to the total count. Raman spectra were collected on a Renishaw system 100 Raman spectrometer using excitation wavelength at 514 nm.

These measurements complemented by additional Raman experiments were obtained between 7 and 400 K using a Kaiser Optical Holospec monochromator in conjunction with a liquid nitrogen cooled CCD detector and a 488 nm Ar laser. Low-temperature spectra were obtained using an Oxford Instruments helium flow cryostat, high-temperature spectra were obtained with the sample capillary kept in a thermostat-controlled metal holder.

The IR spectrum was obtained using a Perkin–Elmer Spectrum One instrument in conjunction with a Golden Gate ATR cell.

3. Results and discussion

3.1. *External vibrations*

Figure 1 presents the low-frequency Raman spectra from 12 to 200 K. At 12 K, many sharp lines are observed. Group theory predicts that in the orthorhombic phase, the librational modes transform as $A_g + 2B_{1g} + B_{2g} + 2B_{3g} + 2A_u + B_{1u} + 2B_{2u} + B_{3u}$, while the translatory optical modes transform as $4A_g + 2B_{1g} + 4B_{2g} + 2B_{3g} + 2A_u + 3B_{1u} + B_{2u} + 3B_{3u}$. All the g modes are Raman active. Miwa et al. [12] have calculated (using plane wave DFT methods) the energy of the zone centre vibrations in $LiBH_4$. Table 1 compares the calculated values with the experimental data at 8 K. These results show a reasonably good agreement between theoretical and experimental values. Racu et al. [11] present low-temperature Raman spectra of $LiBH_4$ and $LiBD_4$ and compare them to new periodic DFT calculations and obtain more detailed assignments of the Raman active modes. There are some small discrepancies between our data and theirs, their experimental resolution and accuracy being slightly better than ours. However, we succeeded to measure three very weak bands above 305 cm^{-1} which were not observed in [11]. The results of [11] are

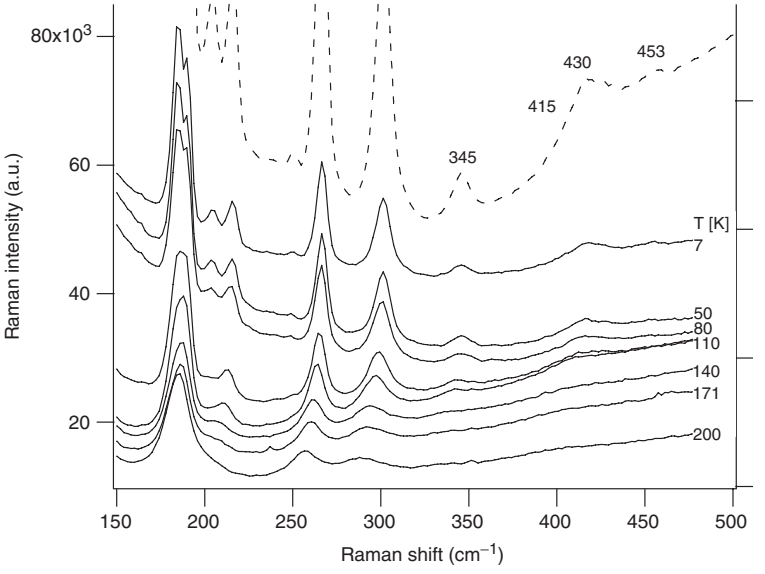

Figure 1. Low-frequency Raman spectra of $LiBH_4$ as a function of temperature between 7 and 200 K. The vertical scale of the 7 K spectrum has been blown up in the dashed trace to show the weak bands above 300 cm^{-1}.

Table 1. Comparison between calculated [11,12] and observed [11 and this work] external (translational and librational) Raman active vibrational frequencies (expressed in cm^{-1}) in $LiBH_4$ (vw = very weak).

Symmetry	Theoretical [12]	Theoretical [11]	Observed (5 K) [11]	Observed (10 K)
B_{1g}	93	125.6		
A_g	107	107	105.6	97 (294 K)
B_{3g}	122	136.6	130.5	
B_{2g}	165	199.6		
B_{3g}	173	155.3	148.8	185
A_g	196	213.3	198	189
B_{1g}	222	212		205
A_g	229	263.3	223.5	216
B_{3g}	234	274.6	257	
B_{1g}	244	290		
B_{2g}	248	276.3	272.7	250 vw
B_{2g}	269	292.3	306.9	267
A_g	280	350.3		302
B_{2g}	340	392		345
B_{3g}	399	439		
B_{2g}	411	455.3		415
B_{1g}	421	459.6		430
A_g	432	483		453

included in Table 1. It is interesting to note that there are some significant differences between the calculated lattice mode frequencies of [11] and [12]: for instance, the A_g modes are calculated at 107, 213.3, 263.3, 350.3 and 483 cm^{-1} in [11] and at 107, 196, 229, 280 and 432 cm^{-1} in [12]. It is not clear whether these differences arise from different

pseudopotentials used, from different calculated lattice constants or other reasons. However, this comparison highlights the difficulties in assigning Raman bands to different symmetry species when polarized spectra cannot be obtained, as large single crystals are not available.

It is important to stress that in $LiBH_4$, the librational modes (which are expected at the highest frequencies of 300–450 cm^{-1}) are potentially coupled to translational motions, as the highest translational bands can also have high frequencies due to the small mass of the Li atom. Thus, the two highest energy external vibrations of B_{2g} symmetry are calculated [12] at 340 and 411 cm^{-1}, of which only one corresponds formally to a librational motion. Hartman et al. [4] have observed by INS bands at *ca* 20, 35 and 52 meV (i.e. 160, 260 and 416 cm^{-1}) and assigned the highest energy band to a librational mode. Racu et al. [11] calculate for these two B_{2g} bands at 455.3 and 392 cm^{-1} isotopic ratios of 1.13 and 1.07 going from $LiBH_4$ to $LiBD_4$, which is very far from the ratio of 1.34 calculated for the highest B_{1g} band at 459.6 cm^{-1}. The next B_{1g} mode is calculated at 290 cm^{-1}, which explains that the 459.6 cm^{-1} band indeed corresponds mainly to a librational motion.

The presence of translational–librational coupling (or mixing) can also be inferred from the low-temperature IR data of $LiBH_4$ and $LiBD_4$ reported by Harvey and McQuaker [8]. They report for $LiBH_4$ IR absorptions at 391, 324 and 274 cm^{-1} and for $LiBD_4$ 340, 276 and 248 cm^{-1} as well as some additional lower frequency bands. One would expect for the pure librational bands an isotopic shift of $1/\sqrt{2}$ going from the hydride to the deuteride. Multiplying the values of 391, 324 and 274 cm^{-1} by this factor, one obtains 277, 230 and 215 cm^{-1}, where only the first value matches the spectrum of $LiBD_4$ and thus corresponds to a librational mode.

The temperature-dependent spectra shown in Figure 1 reveals that above *ca* 80 K, several bands start to broaden and shift to lower frequencies, while others (e.g. around 185 cm^{-1}) remain at the same position. It is important to note that there is no phase transition taking place between 80 and 110 K [5]. The spectra at higher temperatures confirm these trends, but the bands have become too weak and too broad to enable an accurate fitting. However, one may correlate this anomaly with the negative thermal expansion along the *a*-axis below 150 K [5], where according to [7] the free energy should show an additional minimum corresponding to the high-pressure phase. Figure 2 shows the band position *versus* temperature of the two bands observed at 302 and 267 cm^{-1} at 8 K.

Temperature-dependent shifts of vibrational bands are an indication of anharmonic behaviour. In general, the temperature shift of Raman bands in solids can be described by the following expression [13,14]:

$$\omega_j(T) = \omega_j(0) + \Delta\omega_j^{\mathrm{vol}}(T) + \Delta\omega_j^{\mathrm{anh}}(T),$$

or alternatively:

$$\left(\frac{\partial\omega}{\partial T}\right)_p = -\frac{\beta}{\kappa}\left(\frac{\partial\omega}{\partial p}\right)_T + \left(\frac{\partial\omega}{\partial T}\right)_V,$$

where p is the pressure, β the thermal expansion and κ the compressibility.

The contribution $\Delta\omega_j^{\mathrm{vol}}$ accounts for the volume driven effect, while the last term corresponds to the explicit (occupation number driven or amplitude driven) effect. We have applied this equation successfully in the past to describe anharmonicity in the ionic conductor Li_2S [15].

$$\Delta\omega_j^{\mathrm{vol}}(T) = -\int_0^T \frac{\beta}{\kappa}\left(\frac{\partial\omega_j}{\partial p}\right)_T \mathrm{d}T \cong -\frac{1}{\kappa}\left(\frac{\partial\omega_j}{\partial p}\right)_T \int_0^T \beta\,\mathrm{d}T$$

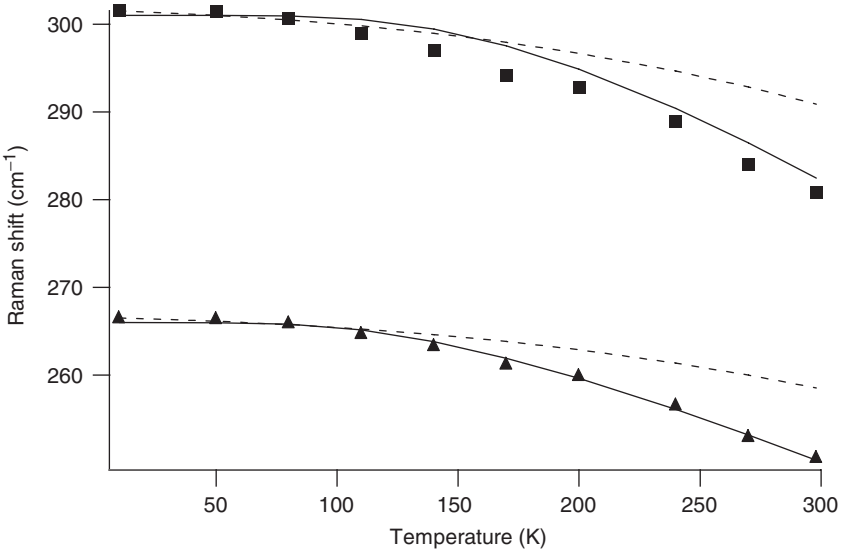

Figure 2. Raman shift *vs.* temperature of the 267 cm^{-1} band and of the 302 cm^{-1} band. The full symbols show the experimental values, the dashed lines corresponds to the calculated shift caused by the volume anharmonicity, the full lines correspond to the fits with explicit mode anharmonicity (see text).

The expression above is valid for cubic crystals, but let us assume that it can also be used in our case. It has been shown for MgF_2 [16] that taking into account lower symmetry effects changes this contribution by 5–15%.

Taking into account the experimental data of the unit cell volume obtained from synchrotron powder diffraction [5]

$$V = 210.85 + 4.78 \times 10^{-3} \cdot T + 2.7 \times 10^{-5} \cdot T^2 + 7.2 \times 10^{-8} \cdot T^3,$$

and assuming that the compressibility and the mode pressure shifts do not change with temperature, we have tried to fit the experimental data as shown in Figure 2 where the calculated band positions using the relations above are shown with a dashed line. This curve was obtained by constraining the fit to the low-temperature data points.

We obtain that $1/\kappa(\partial\omega_j/\partial p)_T = 300$ for the 267 cm^{-1} band and 400 for the 302 cm^{-1} band. Using the value of $B_0 = 14.5$ GPa [6], one can estimate the corresponding pressure shifts of *ca* 20 and 28 cm^{-1} GPa^{-1} for these two modes.

Figure 2 further shows that one cannot neglect additional anharmonic contributions, as there is still a significant discrepancy between observed and calculated band position. Anharmonic couplings with lower energy vibrations can be expressed by [13]:

$$\Delta\omega_j^{\text{anh}} = C\left(n_2 + \frac{1}{2}\right) - D\left[\left(n_3 + \frac{1}{2}\right)^2 + \frac{1}{12}\right] + \frac{2D - 3C}{6},$$

n_2 and n_3 are phonon occupation numbers with half and one-third phonon energy, respectively, than the considered mode, C and D are constants to be adjusted. However, we were not able to obtain a satisfactory fit of the experimental data using this expression.

A more general expression of phonon–phonon creations and destructions is given by [14]:

$$\omega_j(T) = \omega_j(T=0) - \sum_i B_{ji} n_i(T)$$

$$n_i(T) = \frac{1}{e^{\bar{h}\omega_i/kT} - 1}.$$

The terms B_{ji} contain the phonon frequencies and anharmonicities of modes i and j as well as i–j coupling terms. The general resulting temperature dependence can be described by a horizontal part at low temperatures (zero point motion limit) and a linear behaviour at high temperatures. Note that this is approximately the temperature dependence seen in Figure 2.

A different approach to anharmonicity associated with librational motions in molecular crystals has been proposed by Mendonça and Rabbani [17]. Starting from an anharmonic librational oscillator

$$V(\theta) = \frac{1}{2} I\omega_0^2\theta^2 - \lambda\theta^4,$$

where λ is the anharmonic quartic coupling coefficient, they obtain finally (I is the moment of inertia of the molecule):

$$\omega(T) = \omega_0 - \Omega\left[\cot h\left(\frac{\bar{h}\omega_0}{2kT}\right) - 1\right]$$

$$\Omega = \frac{3\bar{h}}{2I^2\omega_0}\lambda.$$

Using this expression, we obtain for the two bands shown in Figure 2 the values of $\omega_0 = 431$ and $326\,\mathrm{cm}^{-1}$ and $\Omega = 65$ and $30\,\mathrm{cm}^{-1}$, respectively. The corresponding temperature variation of these two bands is shown by the full line in Figure 2, and reveals a much better agreement with the experimental data. It is important to note that the two bands considered here are not purely librational modes, as their isotopic ratios (expected to be close to 1.41) are found to be 1.05 ($307\,\mathrm{cm}^{-1}$) and 1.27 ($273\,\mathrm{cm}^{-1}$) at 5 K, as reported by Racu et al. [12] for $LiBH_4$ and $LiBD_4$. Racu et al. [12] identified a strongly anharmonic librational mode (of B_{3g} symmetry) at $149\,\mathrm{cm}^{-1}$. The first harmonic of this mode is close to $300\,\mathrm{cm}^{-1}$, and can thus possibly interact with the $307\,\mathrm{cm}^{-1}$ mode, resulting in the observed anharmonicity.

In the absence of pressure-dependent Raman spectra, it is not possible to quantify the relative contributions of volume-driven and explicit anharmonicity, which are probably very different from mode to mode.

3.2. *Internal vibrations*

Figure 3 presents the Raman spectra in the bending mode region of $LiBH_4$. In their early work, Harvey and McQuaker [8] assigned the weak band at *ca* $1254\,\mathrm{cm}^{-1}$ to the second overtone of a librational band. However, the theoretical vibrational frequencies [11,12] indicate clearly that this band is the third component of the symmetry-split υ_4 deformation mode. This is also corroborated by the relative intensities in the Raman and IR spectra: as can be seen in Figure 3, the intensities of the bands at 1090, 1099 and $1253\,\mathrm{cm}^{-1}$ are much

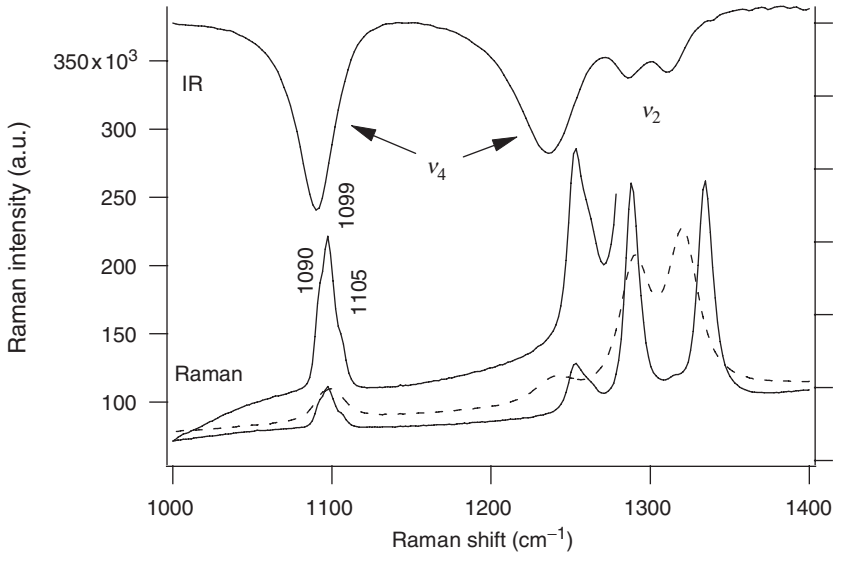

Figure 3. Raman spectra of the deformation modes υ_2 and υ_4 at 12 K (full line) and 300 K (dashed line). The vertical scale of the 12 K spectrum has been expanded to show details of the υ_4 bands. The room temperature IR transmission spectrum is shown in the upper trace.

smaller than those of the bands at 1286 and 1316 cm^{-1}, while it is the opposite in the IR spectrum. At low temperature, a weak additional band at 1105 cm^{-1} can be distinguished, as was also reported in [11].

It is interesting to note that the calculated frequencies of the υ_2 and υ_4 modes are systematically about 30 [11] to 50 cm^{-1} [12] below the experimental values.

Figure 4 presents *in situ* Raman and synchrotron diffraction experiments between 303 and 393 K. The orthorhombic to hexagonal phase transition is clearly observed using both techniques. These new Raman spectra are in perfect agreement with our previously published results [9]. Both probes show a sudden transition, the synchrotron diffraction data also demonstrate a coexistence of both phases, all these observations are indicative of a first-order phase transition. The first-order nature of this transition is also confirmed by the hysteresis observed in the heating and cooling Raman experiment reported previously [9] and agrees with the symmetry analysis [7].

It is interesting to note the temperature evolution of the splitting of the υ_2 mode as a function of temperature, shown in Figure 5. This splitting, which has started to decrease at temperatures above *ca* 100 K, has been reduced from *ca* 47 cm^{-1} at 10 K to *ca* 20 cm^{-1} just below the phase transition. A similar pre-transition feature appears in unit cell dimensions of the orthorhombic cell. Indeed, according to Dimitriev et al. [7] epitaxial relation between Pnma and P6$_3$mc reads as:

$$a_o = c_h, \quad b_o = -(a_h + b_h), \quad c_o = a_h - b_h,$$

where *h*(o) stands for the hexagonal (orthorhombic) cell.

Using these relations, it can be shown that the difference $3b_o^2 - c_o^2$ would become equal to zero for a transition from the Pnma structure to the hexagonal P6$_3$mc. For such a transition, one would also expect the site group of the borohydride ion to evolve from C_s symmetry towards trigonal symmetry, and the site group splitting of the υ_2 mode would tend towards zero, as υ_2 is doubly degenerate in trigonal and higher symmetry.

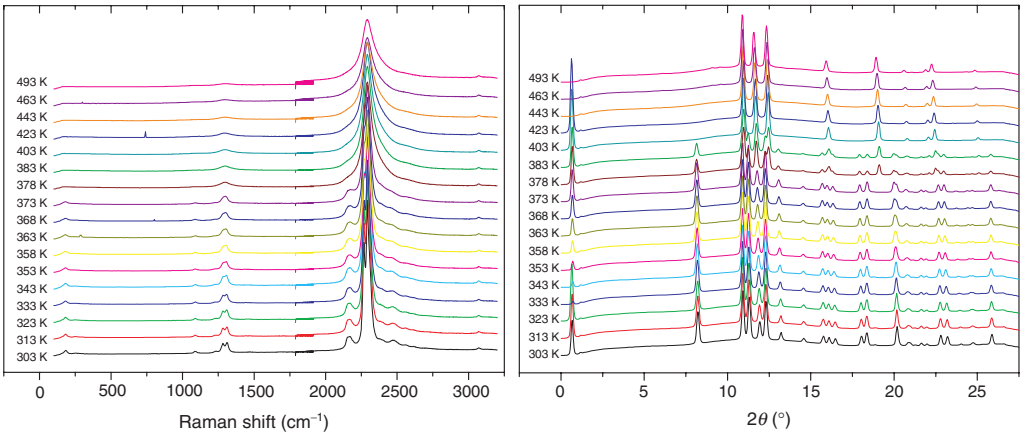

Figure 4. Simultaneous *in situ* Raman (left) and synchrotron diffraction (right) experiments between 303 and 493 K.

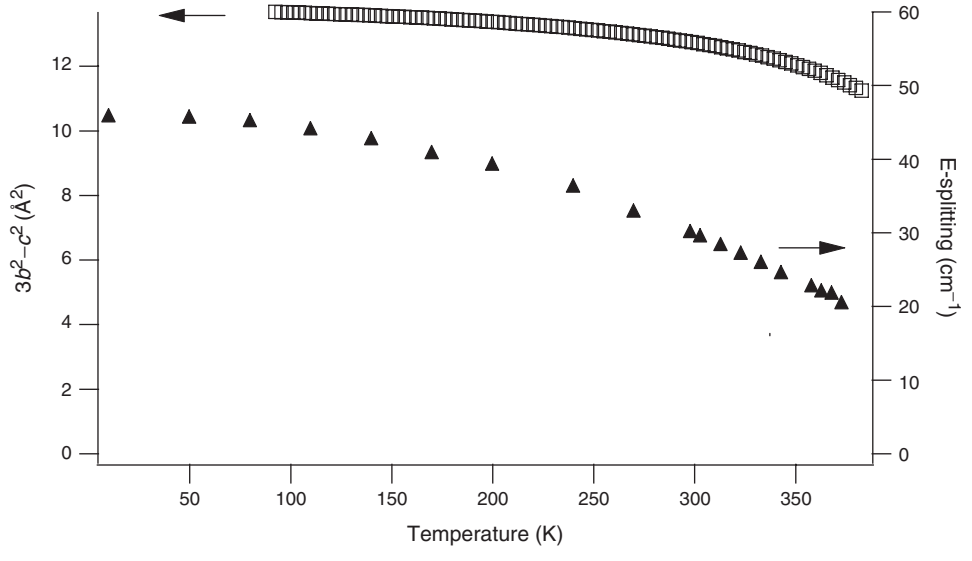

Figure 5. Trend of b and c lattice parameters towards the hexagonal lattice ($3b^2 - c^2 \rightarrow 0$) as a function of temperature (taken from [5], open squares) and temperature dependence of the splitting of the υ_2 mode in the orthorhombic phase (triangles). *In situ* and *ex situ* Raman data have been combined.

Analysis of the temperature dependence of the lattice parameters [5] shows that the difference $3b_o^2 - c_o^2$ decreases between 300 and 380 K (Figure 5), but remains significant at this highest temperature. The surprizing temperature dependence of the b parameter [5] which decreases with increasing temperature between 300 and 360 K (in conjunction with the corresponding increase of the c parameter) can thus be associated with a coupling between the order parameter and spontaneous strain.

As it has been shown in [7], the corresponding order parameter can be parameterized as a shift of layers formed by Li and BH_4, together with in-layer deformations. The temperature dependence of Li–B distances can be, therefore, taken as a probe of inter- and

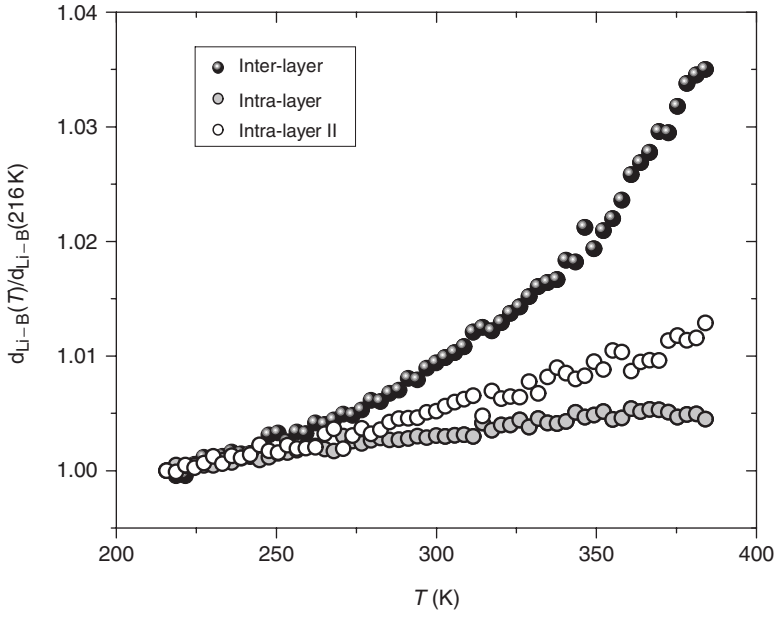

Figure 6. Temperature evolution of intra- and inter-layer Li–B distances. For the definition of layers situated in the *bc* plane of the orthorhombic $LiBH_4$ phase see [7].

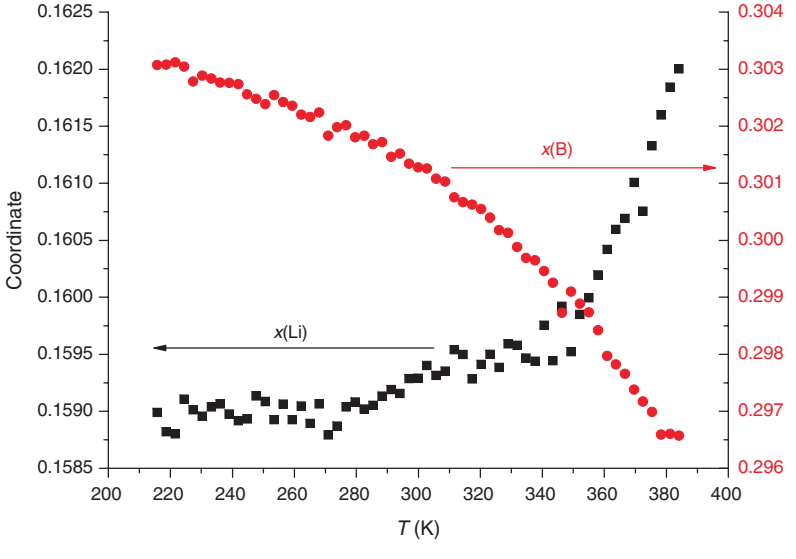

Figure 7. Temperature evolution of *x* coordinates of Li and B atoms, related to the flattening of the Li-BH_4 layers and the anomaly of the unit cell expansion [5] at higher temperatures in the Pnma phase.

intra-layer deformations (Figure 6). Indeed, the layers defined in the *bc* plane of the orthorhombic phase become more flat as the temperature is increased: the difference between atomic coordinates for Li and B atoms decreases with temperature (Figure 7). Also, the distance between the layers increases with temperature (see the inter-layer distance

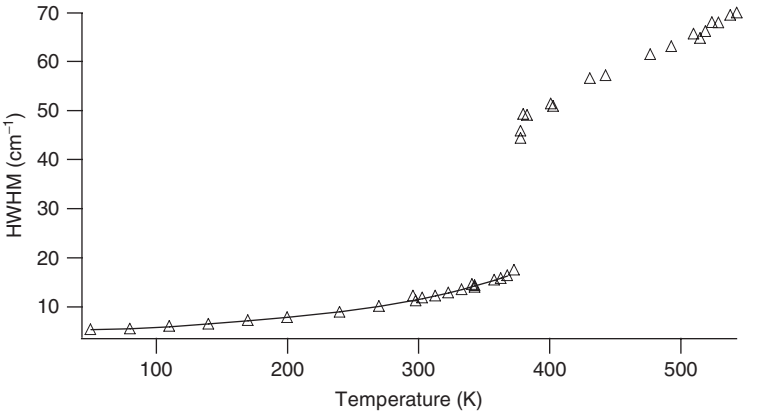

Figure 8. Half-width at half maximum of the υ_2 bands with increasing temperature. Below the phase transition, the average value of the two components is displayed. The solid line corresponds to the biexponential fit of the low temperature data (see text).

in Figure 6). Thus, the thermal evolution of the crystal structure agrees with the phase diagram and description of the order parameters suggested by the Landau theory [7].

Figure 8 illustrates for the entire temperature range the evolution of the linewidth of the υ_2 mode. From 50 to 370 K, the linewidth increases by a factor of about 3. In a previous publication [10], we were able to fit for the cubic crystals MBH_4 (M=Na, K, Rb and Cs) the linewidth *versus* temperature using the simple exponential relation

$$\Gamma = \Gamma_0 + A \cdot e^{-V/RT},$$

where A is a constant and V an activation energy such as the barrier of reorientation. For $LiBH_4$ in the hexagonal phase, this relation did not give a satisfactory fit, and an average value of $15 \pm 2\,\mathrm{kJ\,mol^{-1}}$ was obtained. Using the more complex relation (as one expects several different barriers in a non-cubic crystal)

$$\Gamma = \Gamma_0 + A \cdot e^{-V_1/RT} + B \cdot e^{-V_2/RT},$$

values of 5 ± 5 and $60 \pm 30\,\mathrm{kJ\,mol^{-1}}$ were obtained. The large scatter in these numerical values arises from the restricted temperature range as well as the uncertainty of the determination of the very large linewidth, as seen also by the scatter of the data in Figure 8.

As the data of the low-temperature phase could not be fitted with the simple exponential relation above, the second expression was used to fit to our new data in the orthorhombic phase (Figure 8). Values of $V = 2.9 \pm 0.1$ and $15 \pm 0.5\,\mathrm{kJ\,mol^{-1}}$ were obtained, respectively. The second value is in good agreement with the values of 17.6 ± 0.3 and $24.2 \pm 0.4\,\mathrm{kJ\,mol^{-1}}$ obtained by Skripov et al. [18] from proton and ^{11}B NMR studies. The first very low value agrees with the values observed by Racu et al. [11] for several external and internal modes (in the temperature range from 5 to 300 K) who attributed this low-activation energy to scattering by phonons.

4. Conclusions

The low-frequency Raman spectra of $LiBH_4$ reveal several particular bands which show important shifts as a function of temperature. These shifts are related only in part to

volume driven anharmonicity, intrinsic anharmonicity of the librational modes appears to be the main contribution. These are probably also related to the important dynamic behaviour of the borohydride ion in the low-temperature orthorhombic phase which has been demonstrated previously by neutron diffraction [4]. Pressure-dependent Raman experiments are needed to improve the analysis of the different contributions to anharmonicity in $LiBH_4$.

The evolution of the splitting of the internal υ_2 mode is reminiscent of a pre-transition behaviour which is interrupted by the first-order phase transition. The unusual temperature dependence of the lattice parameters [5] also reflects a trend towards the hexagonal lattice. Splitting of the phonon mode and the lattice strain, both correlate with the atomic shifts parameterized by flattening of Li–B layers and increase of interlayer distance. Such a correlation indicates a coupling of the microscopic order parameter with acoustic and optic phonons and may, as minimum partially, be a reason of a pronounced anharmonicity of some Raman bands.

At the phase transition, the linewidth of the υ_2 (and υ_4) mode increases dramatically, thus revealing additional dynamics in the crystal. At the structural level, the broadening of Raman lines correlates with progressing elongation of inter-layer Li–B contacts, in agreement with the phase transition mechanism suggested by Landau theory [7].

These experimental results, in conjunction with the previous crystallographic studies [3–7], show that $LiBH_4$ presents a complex dynamical behaviour over a broad temperature range in both ambient pressure phases. Current theoretical methods (such as quasi-harmonic DFT calculations) do not allow to reproduce this type of dynamical behaviour, and must be considered 'cum grano sali' when properties of borohydrides are extrapolated to high temperatures.

Acknowledgements

This work was supported by the Swiss National Science Foundation. The authors thank SNBL for the in-house beamtime allocation and Prof. V. Dmitriev for fruitful discussions.

References

[1] M. Au, A. Jurgensen, and K. Zeigler, *Modified lithium borohydrides for reversible hydrogen storage (2)*, J. Phys. Chem. B 110 (2006), pp. 26482–26487.

[2] J. Yang, A. Sudik, and C. Wolverton, *Destabilising $LiBH_4$ with a metal ($M = Mg, Al, Ti, V, Cr,$ or Sc) or metal hydride ($MH_2 = MgH_2$, TiH_2, or CaH_2)*, J. Phys. Chem. C 111 (2007), pp. 19134–19140.

[3] J.-Ph. Soulié, G. Renaudin, R. Černý, and K. Yvon, *Lithium boro-hydride $LiBH_4$. Part 1. Crystal structure*, J. Alloys Comp. 346 (2002), pp. 200–205.

[4] M.R. Hartman, J.J. Rush, T.J. Udovic, R.C. Bowman Jr, and S. Hwang, *Structure and vibrational dynamics of isotopically labeled lithium borohydride using neutron diffraction and spectroscopy*, J. Solid State Chem. 180 (2007), pp. 1298–1305.

[5] Y. Filinchuk, D. Chernyshov, and R. Černý, *Lightest borohydride probed by synchrotron X-ray diffraction: experiment calls for a new theoretical revision*, J. Phys. Chem. C 112 (2008), pp. 10579–10584.

[6] Y. Filinchuk, D. Chernyshov, A. Nevidomskyy, and V. Dmitriev, *High-pressure polymorphism as a step towards destabilization of $LiBH_4$*, Angew. Chem. Int. Ed. 47 (2008), pp. 529–532.

[7] V. Dmitriev, Y. Filinchuk, D. Chernyshov, A.V. Talyzin, A. Dzwilewski, O. Andersson, B. Sundqvist, and A. Kurnosov, *Pressure-temperature phase diagram of $LiBH_4$: Synchrotron X-ray diffraction experiments and theoretical analysis*, Phys. Rev. B 77 (2008), pp. 174112/1–174112/11.
[8] K.B. Harvey and N.R. McQuaker, *Low temperature infrared and Raman spectra of lithium borohydride*, Can. J. Chem. 49 (1971), pp. 3282–3286.
[9] S. Gomes, H. Hagemann, and K. Yvon, *Lithium boro-hydride $LiBH_4$ II. Raman spectroscopy*, J. Alloys Comp. 346 (2002), pp. 206–210.
[10] H. Hagemann, S. Gomes, G. Renaudin, and K. Yvon, *Raman studies of reorientation motions of $[BH_4]^-$ anions in alkali borohydrides*, J. Alloys Comp. 363 (2004), pp. 129–132.
[11] A.-M. Racu, J. Schoenes, Z. Lodziana, A. Borgschulte, and A. Zuttel, *High resolution Raman spectroscopy study of phonon modes in $LiBH_4$ and $LiBD_4$*, J. Phys. Chem. A 112 (2008), pp. 9716–9722.
[12] K. Miwa, N. Ohba, S. Towata, Y. Nakamori, and S. Orimo, *First-principles study on lithium borohydride $LiBH_4$*, Phys. Rev. B 69 (2004), pp. 245120/1–245120/8.
[13] E. Liarokapis, E. Anastassakis, and G.A. Kourouklis, *Raman study of phonon anharmonicity in LaF_3*, Phys. Rev. B 32 (1985), pp. 8346–8355.
[14] R. Zallen and M.L. Slade, *Influence of pressure and temperature on phonons in molecular chalcogenides: crystalline As_4S_4 and S_4N_4*, Phys. Rev. B 18 (1978), pp. 5775–5798.
[15] B. Bertheville, H. Bill, and H. Hagemann, *Experimental Raman scattering investigation of phonon anharmonicity effects in Li_2S*, J. Phys. Condens. Matter 10 (1998), pp. 2155–2169.
[16] A. Perakis, E. Sarantopoulou, Y.S. Raptis, and C. Raptis, *Temperature dependence of Raman scattering and anharmonicity study of MgF_2*, Phys. Rev. B 59 (1999), pp. 775–782.
[17] C. Mendonça and S.R. Rabbani, *Anharmonic lattice vibrations and the temperature shift of Raman spectral lines*, Z. Naturf. A 51 (1996), pp. 716–720.
[18] A.V. Skripov, A.V. Soloninin, Y. Filinchuk, and D. Chernyshov, *Nuclear magnetic resonance study of the rotational motion and the phase transition in $LiBH_4$*, J. Phys. Chem. C 112 (2008), pp. 18701–18705.